Pertanika 13 (3) 395-403 (1990)

An Analytical Two Resistance Mass Transfer Model for Dye Adsorption on Bagasse Pith

G McKAY[1], M.S. El-GEUNDI[1],
M. Z. ABDUL WAHAB and MAMDOUH M. NASSAR[2]
[1]*Department of Chemical Engineering, Queen's University, Belfast BT9 1NN Northern Ireland*
[2]*Department of Chemical Engineering, University of El Minia, El Minia Egypt*

Key words: Analytical Two Resistance Mass Transfer Model, dye adsorption, bagasse pith.

ABSTRAK

Penyerapan empat jenis pewarna iaitu biru berbes 69, merah berbes 22, biru berasid 25 dan merah berasid 114 oleh empular bagas telah dikaji. Model pengangkutan jisim berdasarkan pemindahan jisim luar dan pembauran liang telah digunakan untuk mengaitkan data kepekatan lawan masa yang didapati dari eksperimen dan daripada pengiraan. Model ini adalah penyelesaian analisis yang boleh digunakan dengan sistem penyerapan di mana garisan operasi dan garisan pengikatan berakhir pada dataran penepuan pada isoterma keseimbangan. Satu pekali pemindahan luar jisim dan satu pekali pembauran liang mencukupi untuk menerangkan satu sistem bagi beberapa kepekatan awal pewarna dan beberapa jisim empular. Pekali luar yang didapati bagi pewarna biru berbes 69, merah berbes 22, biru berasid 25 dan merah berasid 114 adalah bersamaan dengan 9.0 x 10^{-3}, 8.0 x 10^{-3}, 1.0 x 10^{-3} dan bagi pewarna-pewarna ini pula masing-masing 5.5 x 10^{-6}, 2.5 x 10^{-6}, 2.2 x 10^{-7} dan 4.5 x 10^{-7} cm^2 s^{-1}.

ABSTRACT

The adsorption of four dyes, namely, Basic Blue 69, Basic Red 22, Acid Blue 25 and Acid Red 114, onto bagasse pith has been studied. A mass transfer model, based on external mass transport and pore diffusion, has been used to correlate experimental and theoretical concentration versus time data. The model is an analytical solution which may be applied to adsorption systems in which the operating line and tie lines all terminate on the saturation plateau of the equilibrium isotherm. A single external mass transfer coefficient and a single pore diffusion coefficient were sufficient to describe each sytem for several initial dye concentrations and several pith masses. The external coefficient were 9.0 x 10^{-3}, 8.0 x 10^{-3}, 1.0 x 10^{-3} and 1.5 x 10^{-3} cm s^{-1}, the pore diffusivities were 5.5 x 10^{-6}, 2.5 x 10^{-6}, 2.2 x 10^{-7} and 4.5 x 10^{-7} cm^2 s^{-1} for Basic Blue 69, Basic Red 22, Acid Blue 25 and Acid Red 114, respectively.

INTRODUCTION

Although several simplified design techniques are available (McKay 1981) for adsorption columns for the wastewater treatment engineer to use, a meaningful design procedure should incorporate the mass transfer processes which are controlling the adsorption step. There are many papers relating to batch or column adsorption processes; some are based on a single resistance to mass transfer, others on two resistance mass transfer. Internal mass transfer is usually considered as either pore diffusion or homogeneous solid phase diffusion. The literature related to these studies has been reviewed in one or two comprehensive papers (Weber and Chakrovorti 1974; Neretnieks 1974).

In order to test fixed bed models, extensive pilot plant tests are necessary, since few of the papers in the literature have developed a model from small scale batch studies which may be extended and applied to the design of fixed bed adsorbers. Some workers have proposed models applicable to both contacting schemes, and for single component (Weber and Lee 1969;

Weber 1978), and multicomponent adsorption (Fritz and Schlunder 1981; Fritz *et al*, 1981). In the work by Spahn and Schlunder (1975), a graphical technique was adopted prior to analytical analysis to obtain an effective pore diffusion coefficient for batch adsorption systems. This procedure was time consuming and sometimes inaccurate due to steep initial gradients on concentration decay curves. A modification to the model proposed by Spahn and Schlunder was developed by McKay (1984) enabling an effective pore diffusion coefficient for batch studies to be obtained rapidly.

The purpose of this paper is to apply the latter model to the adsorption of dyes onto bagasse pith. Pith is a by-product from the sugar industry which is available in great abundance. Much of it is burned directly for energy, though it could be used for adsorption and then combusted. Pith has the ability to adsorb dyestuffs (McKay *et al.* 1987) and the equilibrium isotherms for the adsorption of four dyes, namely, Basic Blue 69, Basic Red 22, Acid Blue 25 and Acid Red 114 have been reported. Furthermore, single resistance mass transfer models were developed for external mass transport or intraparticle diffusion only but when these data were correlated with experimental results, agreement was obtained only over a very limited range of the adsorption period. Consequently, a two resistance model was developed and has been tested for the adsorption of the four dyestuffs onto pith. The influence of two system variables has been investigated namely, initial dye concentration and pith mass.

Theory

Only a brief resume of the theory is presented because all the equations and the mathematical development of the model were reported previously (McKay 1984). The model is based on external mass transfer, pore diffusion and the assumption of an irreversible isotherm.

Providing the operating line terminates at the monolayer, the system can be treated with a "pseudo-irreversible" isotherm approximation, so that

$$q_{e,t} - q_t = q_{e,\,h} - q_t \qquad (1)$$

This allows the use of equation (2) which gives an analytical solution of the form (McKay 1984)

$$\tau = \frac{1}{6C_h}\left[\ln\left(\left|\frac{x^3 + a^3}{1 + a^3}\right|^{2B - \frac{1}{a}}\right)\right] + \ln\left(\left|\frac{x + a}{1 + a}\right|^{3/a}\right) + \frac{1}{(a\sqrt{3})\,C_h}\left[\tan^{-1}\left(\frac{2 - a}{a\sqrt{3}}\right) - \tan^{-1}\left(\frac{2x - a}{a\sqrt{3}}\right)\right] \qquad (2)$$

The derivation procedure is presented in the appendix.

Therefore, by converting dimensionless time, t, into real time, it is possible to compare experimental and theoretical concentration decay curves.

The integration limits for equation (2) are

$$\tau = 0, \quad \eta = 0 \quad \text{and} \quad x = 1 \quad x = a^{0.33}$$
$$\tau = t, \quad \eta = \eta \quad \text{and} \quad x = x$$

The terms in the equation are

$$B = 1 - \underline{(1/Bi)} \qquad (3)$$

$$X = (1 - \eta)^{0.33} \qquad (4)$$

$$a + [(1 - C_h)/C_h]^{0.33} \qquad (5)$$

$$C_h = (W.q_{e,h})/(V.Co) \qquad (6)$$

This model was designed to simulate the behaviour of a batch adsorber using the Spahn and Schlunder model (1975). The analytical solution is similar to that of Neretnieks (1974) and the solution is used for predicting concentration versus time decay curves for the adsorption of dyes onto pith.

The model assumes a pseudo-irreversible (rectangular) isotherm and is only applicable to dye-pith systems in which the operating lines and tie lines terminate on the monolayer (plateau) of the isotherm. This limiting assumption enables a rapid analytical method to be applied for the prediction of concentration versus time decay curves.

The technique enables theoretical data to be compared with experimental results and "best fit" external mass transfer coefficient and effective pore diffusion coefficients to be determined for each dye-pith system. The best fit k_f and D_{eff} values were obtained from minimisation

statistical subroutines incorporated into the programmes.

MATERIALS AND METHODS

Adsorbent

The adsorbent used in this investigation was an Egyptian bagasse pith, kindly provided by Abou-Korkas sugar mill, El-Minia, Egypt. The depithing operation was performed in the sugar mill. The moisture content of bagasse pith was 14.5 ± 0.5%, and it was not subjected to any form of pretreatment prior to use. The pith particles were sieved in the laboratory into various particles size ranges.

The Egyptian bagasse pith was subjected to chemical analysis and the results obtained are a-cellulose, 53.7, pentosan, 27.9, 27.9, lignin, 20.2, alcohol/benzene solubility, 7.5, and ash, 6.6.

Adsorbates

The adsorbates and their structures used in the experiments are listed. The dyestuffs were used as the commercial salts.

(1) Acid Blue 25 (Telon Blue ANL) CI 62055 was supplied by Bayer.

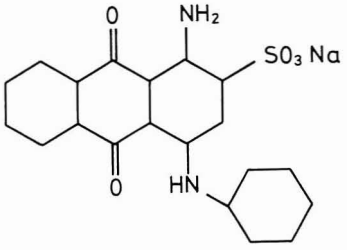

(2) Acid Red 114 (Erionyl Red RS) CI 23635 was supplied by Ciba-Geigy.

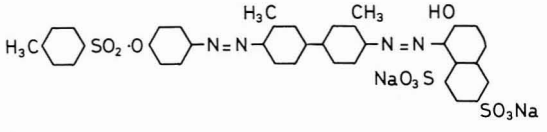

(3) Basic Red 22 (Maxilon Red BL-N) CI 11055 was supplied by Ciba-Geigy.

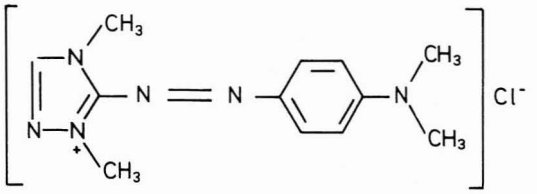

(4) Basic Blue 69 (Astrazone Blue FRR) was supplied by Bayer.

No structure is available for this dye. It belongs to the methine class, of which the chromophore is a conjugate chain of carbon atoms terminated by an ammonium group, and in addition, a nitrogen, sulphur, or oxygen atom, or an equivalent unsaturated group. A general structure for the methine class is

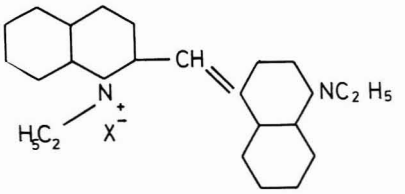

Preparation of Calibration Curve

The dyes were made up in stock solutions of concentration 1000 ppm and were subsequently diluted to required concentrations. Calibration curves for each dye were prepared by recording the absorbance values for a range of known concentrations of dye solution at the wavelength for maximum absorbance of each dye. The value, λ max was found from a full scan of the dye's spectrum and the values are Acid Blue 25, 600 nm, Acid Red 114, 522 nm, Basic Blue 69, 585 nm, and Basic Red 22, 538 nm. These values of λ_{max} were used in all subsequent investigations using the above dyes. All readings and scans were made on a Perkin Elmer Model 550S Spectrophotometer. All tests were carried out at 20± 2°C and dilutions of concentrated solutions were undertaken so that optical densities were measureed in the range 0.1 to 0.6.

Construction of Adsorption Vessel

The standard tank configuration was utilized to obtain the relative dimensions of the vessel and

its components. The following relationships hold with respect to the vessel inside diameter, D_i, see diagram of apparatus.

[1] Li = height of baffles = 20 cm
[2] L2 = baffle width = 0.075 D_i
[3] L3 = height of liquid in the vessel = D_i
[4] L4 = distance between impeller blade and vessel bottom = 0.5 D_i
[5] L5 = width of blade of impeller = 0.1 D_i
[6] L6 = impeller diameter = 0.5 D_i
[7] L7 = impeller shaft diameter = 0.1 D_i

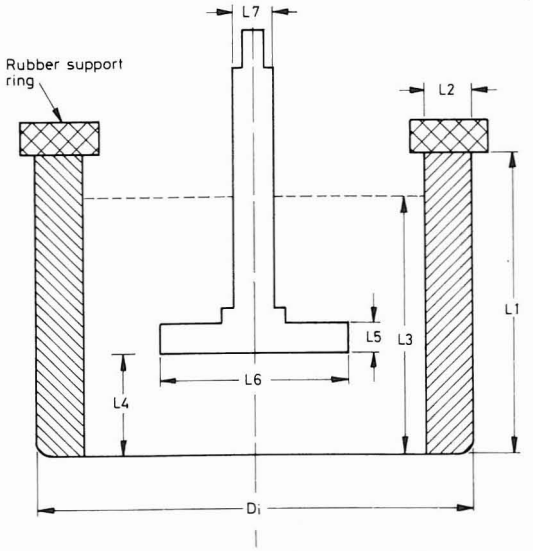

Diagram A. Schematic representation of adsorber vessel.

The adsorber vessel used was a 2 dm^3 glass beaker of internal diameter 0.13 m holding a volume of 1.70 dm^3 dye solution. Mixing was provided by a six bladed, flat stainless steel impeller of 0.065 m diameter and a blade height of 0.013 m. A Heidolph Type 5011 variable speed motor was used to drive the impeller using a 0.013 m diameter stainless steel shaft. Eight anodized aluminium baffles were evenly spaced around the circumference of the vessel, positioned at 45° intervals and held securely in place by insertion into a thick rubber ring placed on top of the vessel. The purpose of the baffles was to prevent the formation of a vortex and the consequential reduction in relative motion, between liquid and solid particles, and power losses due to air entrainment at the impeller. Aluminium baffles were 0.2 m long and 0.01 m wide and were positioned approximately one quarter of the baffle width from the vessel wall and bottom in order to prevent particle accumulation. Evaporation of liquid was prevented by using a thick polythene sheet on top of the rubber ring.

DISCUSSION

The analytical solution to the problem of dye adsorption onto pith can be tested by comparing experimental and theoretical results. Equation (2) has been used to generate concentration decay curves for different D_{eff} and different k_f values.

Initially the value of the external mass transfer coefficient, k_f, was taken from the single resistance analysis value. The independent estimation of the external mass transfer coefficient was obtained using the established technique of Spahn and Schlunder (1975). Consequently this k_f value was used as an initial estimate in the programme and tested using a "best fit" regression analysis method over a wide range of experiments in which pith mass and initial dye concentration were varied.

It is possible to obtain a theoretical decay curve using this value of k_f and an estimation of the effective pore diffusion coefficient, D_{eff}. In order to obtain the theoretical concentration decay curves, the solid phase, η, concentration is abstracted from X in equation (2). It is then possible to obtain the liquid phase concentration, ξ, from the equations in the appendix and theoretical C_t is easily determined from ξ.

By iterating between k_f and D_{eff}, it is possible to obtain a "best fit", again using regression analysis, to the experimental decay curves for batch adsorption.

The model has been applied to four adsorption systems namely, the adsorption of Acid Blue 25, Acid Red 114, Basic Blue 69 and Basic Red 22 onto pith. The value of $q_{e,h}$ adopted in these cases was that of the saturation monolayer coverage of the relevant isotherm. The variables studied were (i) initial dye concentration, and (ii) pith mass.

Figures 1 and *2* show the limiting values of the operating lines at which the analytical model can be used. If it is terminated any more to the

left, the assumption $q_{e,t} = q_{e,h}$ = constant, is invalid and the tie lines will terminate at various values of $q_{e,t}$. In these cases, $C_{e,t}$ is needed to evaluate $q_{e,t}$ and therefore $(dCt/_{dt})$ values are needed.

Figure 3–10 illustrate the fit between the experimental and theoretical results in the form of concentration decay curves by the method outlined earlier. It will be seen that for steep operating lines ending at the adsorption isotherm monolayer, the agreement between theoretical and experimental data is excellent and extends for up to 360 minutes of contact time, but as the operating line approaches the curved region of the isotherm, the agreement between these two methods holds for a short initial interval of time only. This is to be expected as the assumption of pseudo-irreversibility becomes invalid at the curved region of the isotherm.

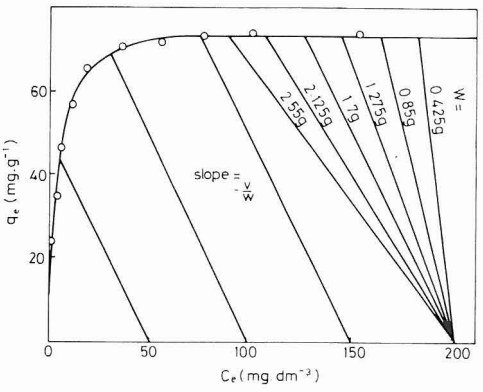

Fig. 1 Equilibrium isotherm for BR22 onto pith showing operating lines at various pith masses and initial dye concentrations.

Based on the theoretical procedure outlined, the rate of adsorption was determined in terms of the two resistances k_f and D_{eff}. The values for these resistance are given in Table 1.

The values of k_f and D_{eff} obtained by Spahn and Schlunder (1975) for another basic dye, Crystal Violet adsorption onto activated carbon are 2.3 x 10^{-3} cm s^{-1} and 5.0 x 10^{-7} cm^2 s^{-1}, respectively. It can be seen that the values in Table 1, compared with those of Spahn and Schlunder (1975) are of a similar order of magnitude.

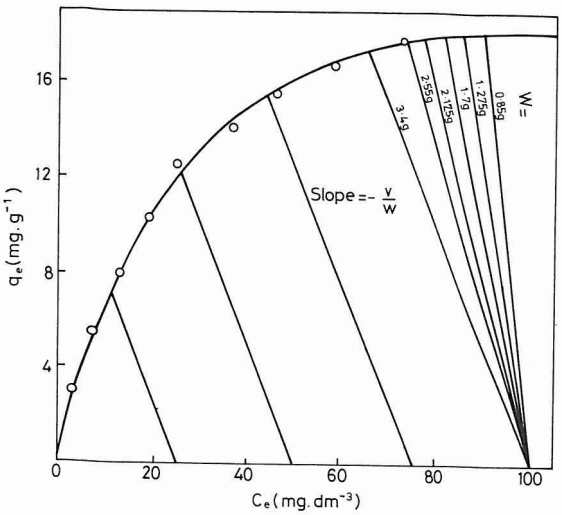

Fig. 2. Equilibrium isotherm for AR114 onto pith showing operating lines at various pith masses and initial dye concentrations.

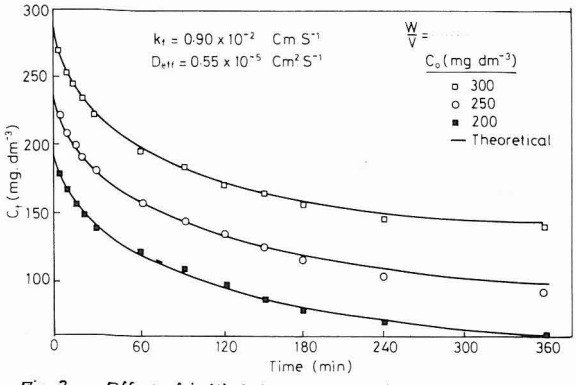

Fig.3. Effect of initial dye concentration on the adsorption of BB69 onto pith using the pore diffusion model. Concentration vs. time curve.

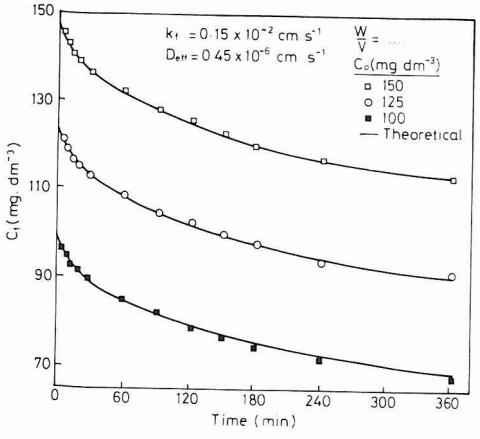

Fig.4. Effect of initial dye concentration on the adsorption of AR114 onto pith using the pore diffusion model. Concentration vs. time curve.

TABLE 1

External Mass Transfer and Effective Pore Diffusion Coefficients for the Adsorption of Dyes onto Pith (Pseudoirreversibility Approximation)

Run No.	Dye	C_o (mg. dm^{-3})	W (g)	g_e, h (mg. g^{-1})	C_h	$k_f \times 10^{-3}$ (cm. s^{-1})	$D_{eff} \times 10^{-7}$ (cm^2. s^{-1})	Bi= $\frac{k_f . R}{D_{eff}}$
1	AB25	100	3.4	21.7	0.434	1.0	2.2	137.5
2		129	3.4	21.7	0.337	1.0	2.2	137.5
3		166	3.4	21.7	0.261	1.0	2.2	137.5
4		100	0.85	21.7	0.109	1.0	2.2	137.5
5		100	1.275	21.7	0.163	1.0	2.2	137.5
6		100	1.7	21.7	0.217	1.0	2.2	137.5
1	AR114	100	3.4	22.9	0.456	1.5	4.5	100.8
2		125	3.4	22.9	0.365	1.5	4.5	100.8
3		150	3.4	22.9	0.304	1.5	4.5	100.8
4		100	0.85	22.9	0.114	1.5	4.5	100.8
5		100	1.275	22.9	1.171	1.5	4.5	100.8
6		100	1.7	22.9	0.228	1.5	4.5	100.8
1	BB69	200	1.7	157.4	0.790	9.0	55.0	49.5
2		250	1.7	157.4	0.632	9.0	55.0	49.5
3		300	1.7	157.4	0.527	9.0	55.0	49.5
4		200	0.425	157.4	0.198	9.0	55.0	49.4
5		200	0.850	157.4	0.395	9.0	55.0	49.5
6		200	1.275	157.4	0.592	9.0	55.0	49.5
1	BR22	200	1.7	76.6	0.384	8.0	25.0	96.8
2		250	1.7	76.6	0.307	8.0	25.0	96.8
3		300	1.7	76.6	0.256	8.0	25.0	96.8
4		200	0.425	76.6	0.096	8.0	25.0	96.8
5		200	0.850	76.6	0.912	8.0	25.0	96.8
6		200	1.275	76.6	0.288	8.0	25.0	96.8

d_p = 605 × 10^{-4} cm, agitation speed = 400 RPM, T = 20°C, V = 1.7 dm^3 and ρ_p = 0.804 g.cm^{-3}.

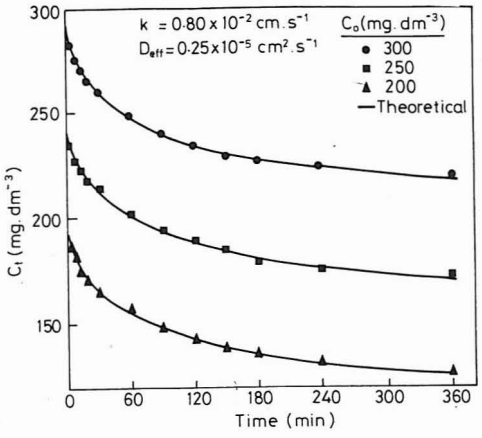

Fig.5. Effect of initial dye concentration on the adsorption of BR22 onto pith using the pore diffusion model. Concentration vs. time curve.

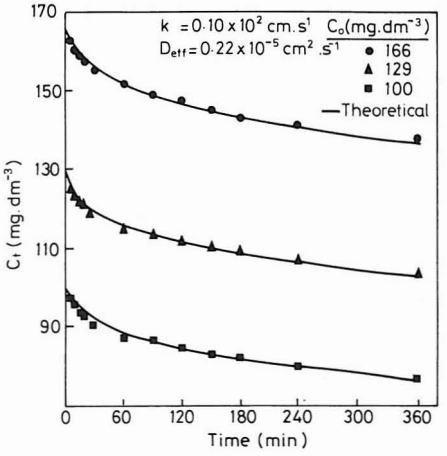

Fig.6. Effect of initial dye concentration on the adsorption of AB25 onto pith using the pore diffusion model. Concentration vs. time curve.

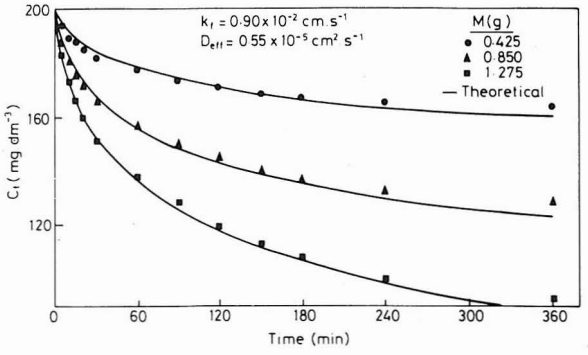

Fig.7. Effect of pith mass on the adsorption of BB69 using the pore diffusion model. Concentration vs. time curve.

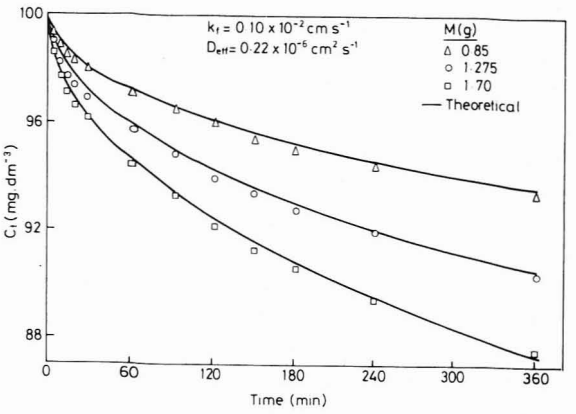

Fig.8. Effect of pith mass on the adsorption of AB25 using the pore diffusion model. Concentration vs. time curve.

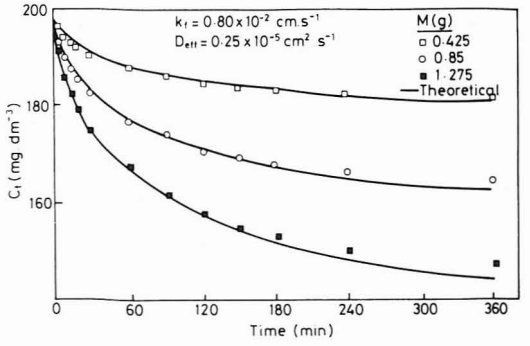

Fig.9. Effect of pith mass on the adsorption of BR22 using the pore diffusion model. Concentration vs. time curve.

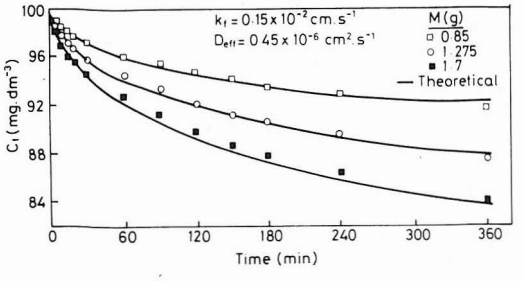

Fig.10. Effect of pith mass on the adsorption of AR114 using the pore diffusion model. Concentration vs. time curve.

For any one dyestuff, a single external mass transfer coefficient and effective pore diffusion coefficient are sufficient to describe that particular system for all variations in pith

masses and initial dye concentrations. The values of the external mass transfer coefficients in Table 1 show considerable variation with variation in dyestuff. Two main reasons are likely for this effect; firstly, the chemical affinity between the different dye ions and pith; secondly, the size of the dye molecule which affects its mobility. The dye ions are large organic molecules and the molecular volumes of Acid Blue 25 and Basic Blue 69 are 690 x 10^{-24} and 650 x 10^{-24} cm^3 molecule $^{-1}$ respectively (McKay 1982). Since the difference between molecular volumes is not large, the difference in k_f values seems largely due to chemical affinity. Pith comprises significant amounts of humic acids which contain phenolic hydroxyl groups and exchange sorption is likely to play an important part in the mechanism.

The variation in effective pore diffusion coefficients in Table 1 describing the internal mass transfer process show a similar relative variation to the external mass transfer coefficients and it would appear that the major controlling factor is the difference in chemical affinity between dye ion and pith. This effect supports the postulated mechanism of pore diffusion since the adsorption affinity is between dye molecules in the solution in the pith pores and the internal sites on the pith.

SUMMARY

A two-resistance model based on external mass transfer and internal pore diffusion has been developed. A pore diffusion model has been used for predicting concentration versus time decay curves for the adsorption of dyes onto pith. The model is restricted to cases where a monolayer equilibrium adsorption is attained. The model has been successfully applied to four adsorption systems, namely, the adsorption of Acid Blue 25, Acid Red 114, Basic Blue 69 and Basic Red 22 onto pith. The method produces excellent correlations between experimental and theoretical concentration decay curves in batch adsorbers. A single external mass transfer coefficient and a single effective pore diffusion coefficient are sufficient to characterise the system within a range of initial dye concentrations, 100 – 300 mg.dm^{-3} and solid/liquid ratios, W/V, 0.25 – 1 g/dm^3. For higher masses, the predicted theoretical curves did not fit the experimental data because the operating and tie lines did not terminate on the monolayer; therefore this analytical model was inapplicable to these systems.

REFERENCES

FRITZ, W. and E.U. SCHLUNDER. 1981. *Chem. Eng. Sci.*, **36**: 721.

FRITZ, W., W. MERK, and E.U. SCHLUNDER 1981. **36**: 731.

McKAY, G. 1981. *Water Research* **31**: 717

McKAY, G. 1982. J. *Chem. Tech. Biotechnol.* **32**: 759.

McKAY, G. 1984. *Chem. Eng. Res. Des.* **62**: 235.

McKAY, G., M.S. EL-GEUNDI, and M.M. NASSAR. 1987. *Water Res.* (In Press) (1987).

NERETNIEKS, I. 1974. *Swedish Paper J.* **77**: 407.

SPAHN, H., and E.U. SCHLUNDER. 1969. *Chem. Eng. Scie.* **30**: 54.

WEBER, T.W., and R.G. LEE, 1969. *Can. J. Chem. Eng.*, **47**: 54.

WEBER, T.W., and R.K. CHAKRAVORTI. 1974. *AIChEJ* **20**, (2): 228.

WEBER. T.W. 1978. *Can. J. Chem. Eng.* **56**: 187 (1978).

(*Received 26 July, 1988*)

NOMENCLATURE

$a = \left[\frac{1 - C_h}{C_h}\right]^{0.33}$ parameter in equation (2)

$B = 1 - \frac{1}{Bi}$, parameter in equation (2)

$Bi = \frac{k_f R}{D_{eff}}$, Biot number

$C_{e,t}$ liquid phase dye concentration at particle surface at time t, mg d^{-3}

C_e, equilibrium liquid phase dye concentration, mg dm^{-3}

$C_h = \frac{W q_{e.h}}{D_{eff}}$, capacity factor

C_o initial liquid phase dye concentration, mg dm^{-3}

d_p pith particle diameter, cm

D_{eff} effective pore diffusivity, cm^2 s^{-1}

k_f external mass transfer coefficient, cm s^{-1}

$q_{e,h}$ equilibrium monolayer saturation ca pacity solid-phase concentration, mg dye g^{-1} pith

q_t mean solid phase concentration at time t, mg dye g^{-1} pith
R particle radius, cm
t contact time
T solution tempertature, °C
V solution volume, dm^3
W pith mass, g
X = $(a - \eta)^{0.33}$, parameter in equation (2)

Greek Letters

η dimensionless solid phase dye concentration, $\frac{q_t}{q_{e,h}}$

ρ_p pith particle density, g cm^{-3}

$\tau = \frac{D_{eff}\, t}{R^2} \cdot \frac{C_o}{\rho_p q_{e,h}}$, dimensionless time

APPENDIX

Theoretical Development

The derivation of equation (2) is outlined in this appendix.

External mass transfer is represented by

$$\dot{N} = A\beta_L (C_t - C_{e,t}) = 4\pi R^2 \beta_L (C_t - C_{e,t}) \quad (7)$$

Mass transfer in the particle is

$$\dot{N} = Ae_s\beta_s(q_{e,t} - \bar{q}_t) \quad (8)$$

The mass balance equation is

$$V(C_o - C_t) = W(\bar{q}_t - q_o) \quad (9)$$

The differential mass balance gives the instantaneous adsorption rate

$$\dot{N}_t = -\frac{VdC_t}{dt} = \frac{Wd\bar{q}_t}{dt} \quad (10)$$

NL can be obtained from the initial adsorption rate

$$\beta_L = -\frac{V}{AC_o}\left(\frac{dC_t}{dt}\right)_{t=0} \quad (11)$$

Having obtained β_L the $C_{e,t}$ and $Q_{e,t}$ may be obtained.

$$C_{e,t} = C_t + \frac{V}{A\beta_L}\left(\frac{dC_t}{dt}\right)_{t=0} \quad (12)$$

For a monolayer isotherm, $q_{e,t}$ is the constant saturation value, thus $\beta_{s,t}$ can be calculated

$$\beta_{s,t} = \frac{\beta_L(C_t - C_{e,t})}{e_s(q_{e,t} - \bar{q}_t)} \quad (13)$$

Now diffusion in a pore of radius r_f is given by Fick's first law:

$$\dot{N} = \frac{4\pi D_{eff} C_{e,t}}{\frac{1}{r_f} - \frac{1}{R}} \quad (14)$$

The velocity of the concentration front in the shrinking pure model is obtained form the mass balance on a spherical element

$$N = \left[\frac{4\pi}{3}(R^3 - r_f^3)e_s\right]q_{e,t} \quad (15)$$

Differentiating gives the adsorption rate:

$$\dot{N} = -4\pi r_f^2 e_s q_{e,t}\frac{dr_f}{dt} \quad (16)$$

Equating equations (7) and (16),

$$\dot{N} = -\pi r_f^2 q_{e,t} e_s \frac{dr^f}{dt} \quad (17)$$

After extensive mathematical development and introducing certain dimensionless groups, the adsorption rate is

$$\frac{d\eta}{d\tau} = \frac{3(1 - C_h\eta)(1 - \eta)^{0.33}}{1 - \left(1 - \frac{1}{Bi}\right)(1 - \eta)}$$

$$\eta = \frac{q_t}{q_{e,t}}, Bi = \frac{\beta_L R}{D_{eff}}, \xi = \frac{C_t}{C_o} \quad (18)$$

$$\eta = 1 - X^3, X = (1 - \eta)^{0.33}, d\eta = -3X^2 dX$$

$$B = 1 - \frac{1}{Bi}, \text{ and } a = \left(\frac{1 - C_h}{C_h}\right)^{0.33}$$

Equation (18) can be integrated to give an analytical solution after simplifying using

$$\tau = \frac{C_o}{e_s q_{e,t}}, \frac{D_{eff}\, t}{R^2}, \xi = 1 - C_h\eta$$

Initially equation (18) becomes

$$-3X^2\frac{dX}{d\tau} = \frac{3[1 - C_h(1 - X^3)]X}{1 - BX} \quad (19)$$

Rearranging

$$d\tau = \frac{X(BX - 1)dX}{1 - C_h(1 - X^3)} \quad (20)$$

A four step integration procedure yields the final result represented by equation (2).